

Effect of electron lateral diffusion in transmission -mode varied-doping $\text{Al}_{0.37}\text{Ga}_{0.63}\text{N}$ photocathode on resolution

HONGGANG WANG^{1,3,*}, XUEHONG JI², DIANLI HOU¹, LILI WANG¹, JINGUANG HAO¹, YAOZHANG SAI¹

¹*School of Information and Electrical Engineering, Ludong University, 264025, Yantai, China*

²*Department of Logistics, Ludong University, 264025, Yantai, China*

³*School of Electronic and Optical Engineering, Nanjing University of Science and Technology, 210094, Nanjing, China*

To achieve a high resolution of transmission-mode $\text{Al}_{0.37}\text{Ga}_{0.63}\text{N}$ photocathode, by establishing the modulation transfer function (MTF) model of this photocathode, we have researched the effect of emission layer thickness T_e , electron diffusion length L_d , recombination velocity at back-interface V_b , and optical absorption coefficient α on MTF of varied-doping and uniform-doping $\text{Al}_{0.37}\text{Ga}_{0.63}\text{N}$ photocathodes. The computational results indicate that the varied-doping structure has a potential in improving both resolution and quantum efficiency of transmission-mode $\text{Al}_{0.37}\text{Ga}_{0.63}\text{N}$ photocathode. This improvement is mainly attributed to the reduction of electron lateral diffusion caused by an electric field which is produced by the varied-doping structure, and thus electron transport towards photocathode surface is facilitated.

(Received July 25, 2021; accepted February 11, 2022)

Keywords: Lateral diffusion, Transmission-mode, Varied-doping, $\text{Al}_{0.37}\text{Ga}_{0.63}\text{N}$ photocathode, Resolution

1. Introduction

In solar-blind ultraviolet detection devices, AlGa_N photocathode has received wide attention [1]. This is mainly attributed to the fact that band gap of AlGa_N crystal material can be increased from 3.42eV to 6.2eV by regulating its Al mole fraction in the range of 0~1, and hence corresponding threshold wavelength decreases from 365nm to 200nm which just meets the needs of solar-blind ultraviolet detection[2]. Naturally, some meaningful work has been reported so far [3-10]. Particularly, solar-blind ultraviolet image intensifier which employs transmission-mode $\text{Al}_{0.37}\text{Ga}_{0.63}\text{N}$ photocathode has been developed [11].

For a transmission-mode $\text{Al}_{0.37}\text{Ga}_{0.63}\text{N}$ photocathode used in solar-blind imaging intensifiers, it must sensitively detect the input light and really transform this optical image to an electron one. So both the quantum efficiency and resolution of AlGa_N photocathode are major considerations. Whereas most research into AlGa_N photocathode has focused on how to improve its quantum efficiency, and very little research has focused on improving its resolution [12-17]. In practice, during the transformation of input light into electrons, some deterioration of resolution is bound to occur in $\text{Al}_{0.37}\text{Ga}_{0.63}\text{N}$ photocathode. Surely, the lateral diffusion of electrons in $\text{Al}_{0.37}\text{Ga}_{0.63}\text{N}$ photocathode accounts for this deterioration. Besides, the current of lateral diffusion is directly proportional to the gradient of electron distribution, and it is denoted by the effect of several photocathode parameters on electron transport towards photocathode surface. If an appropriate electric field whose direction is contrary to that of electron transport towards the surface of $\text{Al}_{0.37}\text{Ga}_{0.63}\text{N}$ photocathode can be formed, the degree of lateral diffusion of electrons will be

suppressed. As a result, the deterioration of resolution may be offset to some extent.

Interestingly, the negative electron affinity photocathode (NEA) based on varied-doping structure is capable of forming this electric field [18]. Figs. 1 and 2 show that varied-doping structure forms a bent-band region sloping linearly downwards and hence generates a constant electric field F . More convincingly, the varied-doping NEA photocathode has obtained higher quantum efficiency than the uniform-doping counterpart, which has been verified by J. J. Zou, and Xiaohui Wang, et al [19, 20]. Therefore, the transmission-mode varied-doping $\text{Al}_{0.37}\text{Ga}_{0.63}\text{N}$ photocathode has the potential in achieving high resolution and high quantum efficiency, since the lateral diffusion of electrons in this photocathode can be suppressed. As shown in Fig.3, the diameter of lateral diffusion for a varied-doping $\text{Al}_{0.37}\text{Ga}_{0.63}\text{N}$ photocathode appears smaller than that for a uniform-doping one owing to the addition of electric field F , stated another way, the resolution of photocathode is increased. Consequently, it is important to discuss the effect of electron lateral diffusion in transmission-mode $\text{Al}_{0.37}\text{Ga}_{0.63}\text{N}$ photocathode on resolution. From the standpoint of structural design of photocathodes, it is more significant to study the dependence of resolution on emission layer thickness T_e , electron diffusion length L_d , optical absorption coefficient α , and recombination velocity at back-interface V_b . Resultantly, the intent of this paper is to study the influence of electron lateral diffusion in transmission-mode varied-doping and uniform-doping $\text{Al}_{0.37}\text{Ga}_{0.63}\text{N}$ photocathodes on their resolution by way of discussing the dependence of resolution on T_e , L_d , V_b , and α . Simultaneously, we will discuss the relationship between

resolution and quantum efficiency of $\text{Al}_{0.37}\text{Ga}_{0.63}\text{N}$ photocathode.

2. Model of modulation transfer function

A typical evaluation of resolution characteristics of an image intensifier is modulation transfer function (MTF), and it is logical for a transmission-mode varied-doping $\text{Al}_{0.37}\text{Ga}_{0.63}\text{N}$ photocathode as well [21]. In a bid to clarify the effect of electron lateral diffusion on the resolution of photocathode, it is necessary to establish an appropriate MTF model of transmission-mode varied-doping $\text{Al}_{0.37}\text{Ga}_{0.63}\text{N}$ photocathode.

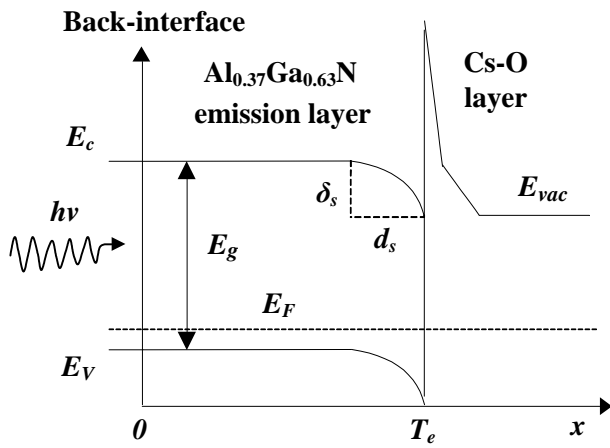


Fig. 1. Band schematic diagram of a transmission-mode uniform-doping $\text{Al}_{0.37}\text{Ga}_{0.63}\text{N}$ photocathode. E_c is conduction-band minimum, E_v is valence-band maximum, E_g is band gap, E_F is Fermi level, δ_s and d_s are height and width of the bent-band region, respectively, and E_{vac} is vacuum level

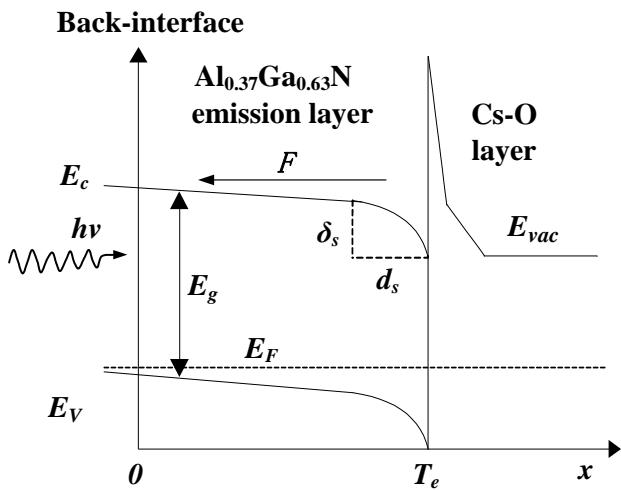


Fig. 2. Band schematic diagram of a transmission-mode varied-doping $\text{Al}_{0.37}\text{Ga}_{0.63}\text{N}$ photocathode. F is the strength of electric field. The meanings of all other parameters are the same as Fig. 1

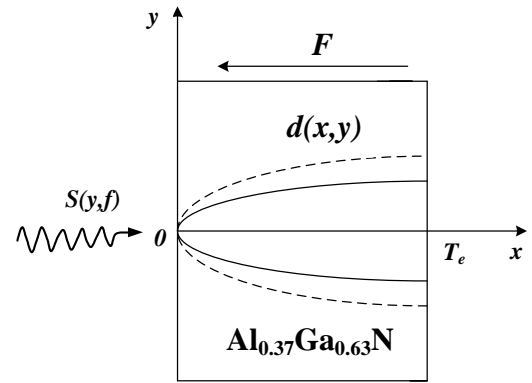


Fig. 3. Schematic diagram of electron lateral diffusion in $\text{Al}_{0.37}\text{Ga}_{0.63}\text{N}$ photocathode. Solid line defines electron lateral diffusion with a constant electric field F ; dashed line represents electron lateral diffusion without F

As shown in Fig. 3, suppose that there is a beam of input light that is perpendicular to the substrate of a transmission-mode varied-doping $\text{Al}_{0.37}\text{Ga}_{0.63}\text{N}$ photocathode, and the light intensity $S(y,f)$ takes the form of

$$S(y, f) = \frac{\phi}{2} [1 + \cos(2\pi fy)] \quad (1)$$

where ϕ is the flux of input light, and f denotes the spatial frequency whose units are lp/mm. Because of electric field F caused by varied-doping structure, the electron diffusion expression representing the generation of electrons and their transport towards NEA surface is defined as

$$\frac{\partial^2 d(x, y)}{\partial x^2} + \frac{\partial^2 d(x, y)}{\partial y^2} - \frac{q|F|}{kT} \frac{d(x, y)}{L_d} + \frac{G(x, y)}{D_n} = 0 \quad (2)$$

$(x \in [0, T_e], y \in \text{Real})$

where x is the distance between a point inside emission layer of $\text{Al}_{0.37}\text{Ga}_{0.63}\text{N}$ photocathode and its surface, $d(x,y)$ denotes electron density, q represents electronic charge, k is Boltzmann's constant, T is temperature, L_d stands for electron diffusion length, D_n denotes electron diffusion coefficient, T_e states emission layer thickness, and $G(x,y)$ defines electron generation function. Specially, $G(x,y)$ is given by

$$G(x, y) = \alpha(1 - R) \exp(-\alpha x) S(y, f) \quad (3)$$

where α is optical absorption coefficient, and R denotes the reflectivity at $\text{Al}_{0.37}\text{Ga}_{0.63}\text{N}$ photocathode surface. And then the boundary condition of Eq.(2) is determined by

$$D_n \left[\frac{\partial d(x, y)}{\partial x} - \frac{q|F|}{kT} d(x, y) \right]_{x=0} = V_b d(x, y)|_{x=0}, \quad (4)$$

$$d(x, y)|_{x=T_e} = 0$$

where V_b is recombination velocity at photocathode back-interface. For solving Eq.(2), it is fundamental to perform Fourier transformation with respect to y when y is a real number. Assuming that Fourier transformation of $d(x, y)$ as

$$F[d(x, y)] = Z(x, \lambda) \quad (5)$$

we can obtain corresponding second-order differential equation in regard to x as follows

$$D_n \left[\frac{d^2 Z(x, \lambda)}{dx^2} - \frac{q|F|}{kT} \frac{dZ(x, \lambda)}{dx} - \left(\lambda^2 + \frac{1}{L_d^2} \right) Z(x, \lambda) \right] + \alpha(1-R)\exp(-\alpha x) \cdot \left[\sqrt{2\pi} \delta(\lambda) + \sqrt{\frac{\pi}{2}} (\delta(\lambda + \omega) + \delta(\lambda - \omega)) \right] = 0 \quad (6)$$

and then the boundary condition of Eq.(6) is given by

$$\left[D_n \frac{dZ(x, \lambda)}{dx} - \frac{q|F|}{kT} Z(x, \lambda) \right]_{x=0} = V_b Z(x, \lambda)|_{x=0}, \quad Z(x, \lambda)|_{x=T_e} = 0 \quad (7)$$

Subsequently, by solving Eq.(6) for $Z(x, \lambda)$ and performing inverse Fourier transformation, the photocurrent density expression $J_T(y, f)$ of a transmission-mode varied-doping $\text{Al}_{0.37}\text{Ga}_{0.63}\text{N}$ photocathode can be obtained, and it is given by

$$J_T(y, f) = -PD_n \frac{\partial d(x, y)}{\partial x} \Big|_{x=T_e} = \frac{\phi}{2} [Y_{T_0} + Y_{T_\omega} \cos(2\pi fy)] \quad (8)$$

where P is electron escape probability at photocathode surface, Y_{T_0} defines the quantum efficiency of photoemission caused by input light with homogeneous distribution, and Y_{T_ω} defines the quantum efficiency of photoemission caused by input light with cosinusoidal distribution. Concretely, both expressions are determined by

$$Y_{T_0} = \frac{P(1-R)\alpha L_d}{\alpha^2 L_d^2 + \alpha L_\omega - 1} \cdot \left\{ \frac{N_\omega (V + \alpha D_n) \exp\left(\frac{L_\omega T_e}{2L_d^2}\right) - Q_\omega \exp(-\alpha T_e)}{M_\omega} - \alpha L_d \exp(-\alpha T_e) \right\} \quad (9)$$

$$Y_{T_\omega} = \frac{P(1-R)\alpha L_d}{\alpha^2 L_d^2 + \alpha L_\omega - 1} \cdot \left\{ \frac{N_\omega (V + \alpha D_n) \exp\left(\frac{L_\omega T_e}{2L_d^2}\right) - Q_\omega \exp(-\alpha T_e)}{M_\omega} - \alpha L_d \exp(-\alpha T_e) \right\} \quad (10)$$

where,

$$L_\omega = \frac{q|F|}{kT} L_d^2, \quad V = V_b + \frac{q|F|}{kT} D_n, \quad N_\omega = \sqrt{L_\omega^2 + 4L_d^2},$$

$$M_\omega = \frac{N_\omega D_n}{L_d} \cosh\left(\frac{N_\omega T_e}{2L_d^2}\right) + \left(2VL_d - \frac{L_\omega D_n}{L_d}\right) \sinh\left(\frac{N_\omega T_e}{2L_d^2}\right),$$

$$Q_\omega = VN_\omega \cosh\left(\frac{N_\omega T_e}{2L_d^2}\right) + (VL_\omega + 2D_n) \sinh\left(\frac{N_\omega T_e}{2L_d^2}\right),$$

$$L_d' = \sqrt{\frac{L_d^2}{L_d^2 \omega^2 + 1}}, \quad L_\omega = \frac{q|F|}{kT} L_d'^2, \quad N_\omega = \sqrt{L_\omega'^2 + 4L_d'^2},$$

$$M_\omega = \frac{N_\omega D_n}{L_d'} \cosh\left(\frac{N_\omega T_e}{2L_d'^2}\right) + \left(2VL_d' - \frac{L_\omega D_n}{L_d'}\right) \sinh\left(\frac{N_\omega T_e}{2L_d'^2}\right),$$

$$Q_\omega = VN_\omega \cosh\left(\frac{N_\omega T_e}{2L_d'^2}\right) + (VL_\omega + 2D_n) \sinh\left(\frac{N_\omega T_e}{2L_d'^2}\right).$$

In fact, the definition of MTF is governed by the ratio of J_{T_ω} to J_{T_0} . Concerning the image formed by the light with cosine distribution at a certain spatial frequency, where J_{T_ω} and J_{T_0} are the contrast of this image plane and that of the objective plane, respectively. In the case of a transmission-mode $\text{Al}_{0.37}\text{Ga}_{0.63}\text{N}$ photocathode, J_{T_0} is actually the contrast of photoemission current density. Accordingly, the MTF model of this transmission-mode varied-doping $\text{Al}_{0.37}\text{Ga}_{0.63}\text{N}$ photocathode is given by

$$MTF_T(f) = \frac{J_{T_\omega}}{J_{T_0}} = \frac{Y_{T_\omega}}{Y_{T_0}} \quad (11)$$

More specially, substituting formulas (9) and (10) into formula (11), we can establish this model as

$$MTF_T(f) = \frac{L_d' M_\omega (\alpha^2 L_d'^2 + \alpha L_\omega - 1)}{L_d M_\omega (\alpha^2 L_d^2 + \alpha L_\omega - 1)} \cdot \left[\frac{N_\omega (V + \alpha D_n) \exp\left(\frac{L_\omega T_e}{2L_d^2}\right) - Q_\omega \exp(-\alpha T_e) - M_\omega \alpha L_d \exp(-\alpha T_e)}{N_\omega (V + \alpha D_n) \exp\left(\frac{L_\omega T_e}{2L_d'^2}\right) - Q_\omega \exp(-\alpha T_e) - M_\omega \alpha L_d' \exp(-\alpha T_e)} \right] \quad (12)$$

In addition, if electric field F is zero in Eq.(4), the MTF model of a transmission-mode uniform-doping $\text{Al}_{0.37}\text{Ga}_{0.63}\text{N}$ photocathode can be easily obtained. According to the physical meaning of MTF, the value of MTF changes in the range of 0~1. In general, the larger

MTF indicates the higher image quality, in other words, the higher resolution of this photocathode.

3. Results and discussions

Prior to studying MTF characteristics of transmission-mode varied-doping Al_{0.37}Ga_{0.63}N photocathode, some essential computational conditions must be determined. These conditions are given that the quantity of band-bending caused by varied-doping structure is 0.06eV when the doping level increases from $2.5 \times 10^{18} \text{ cm}^{-3}$ to $2.5 \times 10^{19} \text{ cm}^{-3}$, $P=0.38$, $R=0.21$, and $D_n=6.25 \text{ cm}^2/\text{s}$ at room temperature [22, 23]. Combining these values with MTF model, we have calculated MTF of transmission-mode varied-doping and uniform-doping Al_{0.37}Ga_{0.63}N photocathodes, and then comparatively researched both resolution characteristics. More concretely, the effect of emission layer thickness T_e , electron diffusion length L_d , recombination velocity at back-interface V_b , and optical absorption coefficient α on resolution and quantum efficiency are researched. By changing T_e , L_d , V_b , and α respectively, a family of MTF curves are plotted and these curves accompanied with corresponding values of quantum efficiency when spatial frequency f is in the range of 0~1600 lp/mm are shown in Fig.4, Fig.5, Fig.6, and Fig.7.

The most obvious properties in these figures is that all MTF curves drop off when f is increased, which is mainly related to the degree of electron lateral diffusion. Clearly, the MTF is a monotonically decreasing function of f . For a constant f , the substantial embodiment of the influence of electron lateral diffusion on resolution is the dependence of MTF on T_e , L_d , V_b , and α . What's particularly important is the ability of varied-doping structure to improve the resolution of Al_{0.37}Ga_{0.63}N photocathode in most cases, compared with the uniform-doping counterpart. Subsequently, we discuss the effect of T_e , L_d , V_b , and α on resolution. Meanwhile, the matching quantum efficiency Y_{TV} of a transmission-mode varied-doping Al_{0.37}Ga_{0.63}N photocathode and quantum efficiency Y_{TU} of a transmission-mode uniform-doping Al_{0.37}Ga_{0.63}N photocathode are given.

3.1. Effect of T_e on resolution

Assuming $L_d=1.0 \text{ }\mu\text{m}$, $\alpha=3 \times 10^4 \text{ cm}^{-1}$, and $V_b=0 \text{ cm}\cdot\text{s}^{-1}$, the MTF curves of transmission-mode varied-doping and uniform-doping Al_{0.37}Ga_{0.63}N photocathode are plotted in Fig.4 when $T_e=0.3 \text{ }\mu\text{m}$ and $0.6 \text{ }\mu\text{m}$, respectively. As can be seen from Fig.4, MTF of both Al_{0.37}Ga_{0.63}N photocathodes rise dramatically when emission layer thickness T_e is reduced. Particularly, the MTF of varied-doping Al_{0.37}Ga_{0.63}N photocathode rises more markedly. It is well illustrated by the fact that a small T_e will suppress electron lateral diffusion owing to the reduction of diffusion distance. From the standpoint of electron transport, a smaller T_e will form a stronger electric field F and hence easily promote electron transport. Conversely, a lower quantum efficiency will be produced by a smaller T_e at short wavelengths. In addition, for a given transmission-

mode Al_{0.37}Ga_{0.63}N photocathode, the influence of T_e on quantum efficiency at different wavelengths is different. For example, in the case of a small T_e , the spectral response at short wavelengths increases, whereas the spectral response at long wavelengths decreases. Inversely, for a very large T_e , quantum efficiency at full wavelengths region decreases and the influence of electric field produced by varied-doping structure appears weak. Therefore, the determination of an optimal thickness of emission layer T_{em} is crucial in combining quantum efficiency with resolution for a transmission-mode varied-doping Al_{0.37}Ga_{0.63}N photocathode.

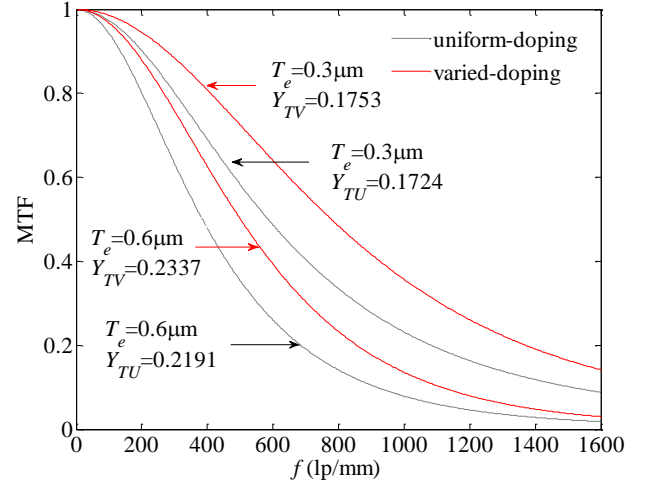


Fig. 4. Effect of T_e on resolution of transmission-mode varied-doping and uniform-doping Al_{0.37}Ga_{0.63}N photocathodes (color online)

3.2. Effect of L_d on resolution

When $T_e=0.5 \text{ }\mu\text{m}$, $\alpha=3 \times 10^4 \text{ cm}^{-1}$, and $V_b=0 \text{ cm}\cdot\text{s}^{-1}$, we have plotted MTF curves of transmission-mode varied-doping and uniform-doping Al_{0.37}Ga_{0.63}N photocathode for $L_d=0.5 \text{ }\mu\text{m}$ and $1.0 \text{ }\mu\text{m}$, and it is shown in Fig. 5. Clearly, it is found that all MTF curves rise with shortening electron diffusion length L_d , but the corresponding values of quantum efficiency is reduced. More specially, the MTF of uniform-doping Al_{0.37}Ga_{0.63}N photocathode rises more markedly. For instance, when spatial frequency f is 800lp/mm, the MTF values of varied-doping photocathode are 0.3799 and 0.2804 for $L_d=0.5 \text{ }\mu\text{m}$ and $1.0\mu\text{m}$, respectively, i.e., it increases by 35.49%. Whereas the MTF values of uniform-doping Al_{0.37}Ga_{0.63}N photocathode are 0.342 and 0.1883, respectively, i.e., it increases by 81.63%.

At the same time, it is noted that both MTF have little deviation as $L_d=0.5 \text{ }\mu\text{m}$, but the deviation becomes large as $L_d=1.0 \text{ }\mu\text{m}$. Stated another way, the shorter L_d can give rise to the smaller influence on both MTF. This discrepancy is attributed to the fact that the degree of electron lateral diffusion is minimized with shortening L_d , since most electrons escaping into vacuum come from the region near photocathode surface. Accordingly, the effect of electric field formed by varied-doping structure is gradually weakened with shortening L_d . However, it should be noticed that a short L_d will lead to a high resolution but result in a low quantum efficiency.

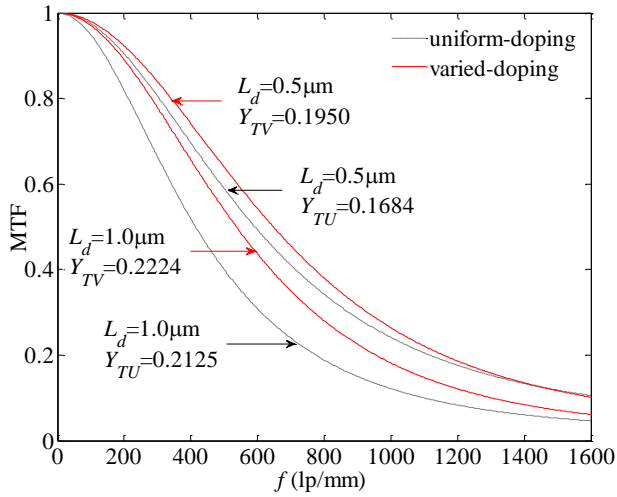


Fig. 5. Effect of L_d on resolution of transmission-mode varied-doping and uniform-doping $\text{Al}_{0.37}\text{Ga}_{0.63}\text{N}$ photocathodes (color online)

3.3. Effect of V_b on resolution

In a bid to research the effect of recombination velocity at back-interface V_b on resolution of transmission-mode varied-doping and uniform-doping $\text{Al}_{0.37}\text{Ga}_{0.63}\text{N}$ photocathodes, we give MTF of both photocathodes in the case of $T_e=0.5 \mu\text{m}$, $L_d=1.0 \mu\text{m}$, and $\alpha=3 \times 10^4 \text{ cm}^{-1}$, via changing $V_b=0 \text{ cm}\cdot\text{s}^{-1}$ and $V_b=10^7 \text{ cm}\cdot\text{s}^{-1}$, individually. As shown in Fig.6, it is clear that the higher V_b leads to higher resolution for both photocathodes. As $V_b=10^7 \text{ cm}\cdot\text{s}^{-1}$, the resolution characteristics of both photocathodes are nearly identical, namely, varied-doping structure cannot improve resolution because of the recombination of most electrons. For $V_b=0 \text{ cm}\cdot\text{s}^{-1}$, electrons are entirely reflected from the back-interface, and thus most of emitted electrons diffuse further laterally as a result of a longer diffusion distance, which can be suppressed by electric field for varied-doping $\text{Al}_{0.37}\text{Ga}_{0.63}\text{N}$ photocathode.

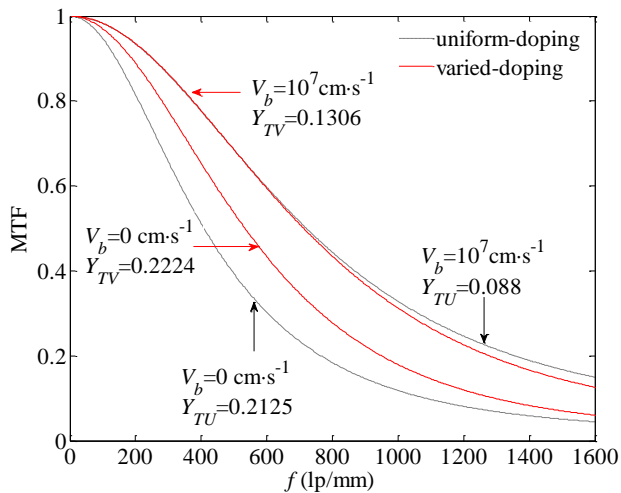


Fig. 6. Effect of V_b on resolution of transmission-mode varied-doping and uniform-doping $\text{Al}_{0.37}\text{Ga}_{0.63}\text{N}$ photocathodes (color online)

Therefore, for a low V_b , the resolution of varied-doping $\text{Al}_{0.37}\text{Ga}_{0.63}\text{N}$ photocathode is distinctly higher than that of uniform-doping one. For a high V_b (equal to or higher than $10^7 \text{ cm}\cdot\text{s}^{-1}$), the majority of electrons reaching the back-interface will be recombined and then lost, i.e., the influence of electric field is neglected. Accordingly, the suppression of electric field on electron lateral diffusion appears trivial. Nevertheless, a high resolution is obtained at the expense of a reduction in quantum efficiency with raising V_b , and this reduction is induced by those emitted electrons improving resolution.

3.4. Effect of α on resolution

As $T_e=0.5 \mu\text{m}$, $L_d=1.0 \mu\text{m}$, and $V_b=0 \text{ cm}\cdot\text{s}^{-1}$, the MTF curves of transmission-mode varied-doping and uniform-doping $\text{Al}_{0.37}\text{Ga}_{0.63}\text{N}$ photocathodes have been plotted in Fig.7 by assuming $\alpha=3 \times 10^4 \text{ cm}^{-1}$ and $\alpha=6 \times 10^4 \text{ cm}^{-1}$, respectively. As can be seen from Fig.7, it is obvious that the MTF of both photocathodes fall as optical absorption coefficient α is increased. This is mainly because that more electrons are produced near photocathode back-interface with increasing α . With a high α , electrons have a longer diffusion distance towards photocathode surface, in another word, these electrons diffuse more laterally. In the meanwhile, when emission layer thickness T_e is smaller than its optimal value T_{em} which is crucial parameter in developing transmission-mode photocathode, the corresponding quantum efficiency increases as α is increased owing to the increased number of excited electrons, most of these electrons are able to escape into vacuum. If T_e is larger than T_{em} , the quantum efficiency decreases with increasing α . This is explained as follows. On the one hand, for a small α , light absorption is approximately uniform throughout the $\text{Al}_{0.37}\text{Ga}_{0.63}\text{N}$ photocathode, which implies that there is a substantial number of electrons produced within diffusion length. When α is increased, fewer electrons are produced near the photocathode surface. On the other hand, if α is small, there are multiple internal reflections and thus can increase the number of electrons produced near photocathode surface. Furthermore, with increasing α , this increment decreases.

As discussed above, it is evident that varied-doping structure can improve resolution of transmission-mode $\text{Al}_{0.37}\text{Ga}_{0.63}\text{N}$ photocathode with the exception of a very large recombination velocity at back-interface V_b . We attribute this improvement mainly to the fact that electron lateral diffusion in transmission-mode varied-doping $\text{Al}_{0.37}\text{Ga}_{0.63}\text{N}$ photocathode is suppressed by electric field F , i.e., F promotes electron transport towards photocathode surface. Moreover, it should be noted that simultaneous achievement of high resolution and high quantum efficiency for a transmission-mode varied-doping $\text{Al}_{0.37}\text{Ga}_{0.63}\text{N}$ photocathode is clearly different from the achievement of high resolution for a transmission-mode uniform-doping one. To be more specific, the latter is obtained by reducing T_e and L_d or raising V_b which lead to a low quantum efficiency. What's more, the actual selection of T_e , L_d , V_b , and α is by no means arbitrary. As an example, for a practical $\text{Al}_{0.37}\text{Ga}_{0.63}\text{N}$ photocathode, V_b is dominated

by the defect at back-interface, and this defect is mainly caused by the mismatching dislocation between buffer layer and emission layer. In other words, an effective approach to obtaining a smaller V_b is reducing the density of mismatching dislocation. Additionally, L_d is deduced by fitting experimental curves of quantum efficiency of the photocathode sample. If L_d cannot satisfy the requirements, it may be optimized via the variation of doping concentration. Therefore, the compatibility of high resolution and high quantum efficiency will not be achieved by the change in these parameters. Naturally, a compromise must be made in reality.

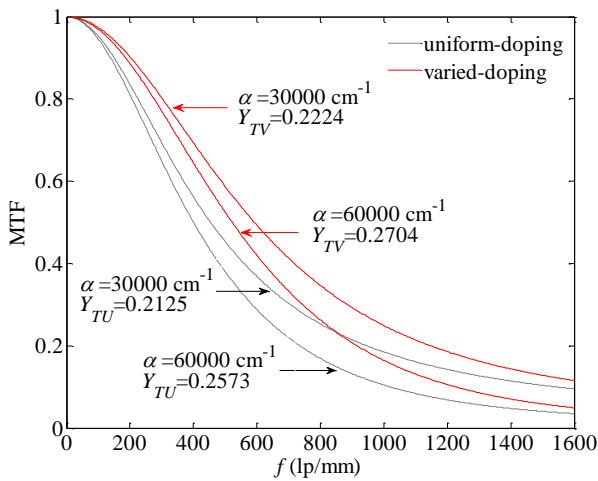


Fig. 7. Effect of α on resolution of transmission-mode varied-doping and uniform-doping $\text{Al}_{0.37}\text{Ga}_{0.63}\text{N}$ photocathodes (color online)

4. Conclusions

Resolution of a transmission-mode varied-doping $\text{Al}_{0.37}\text{Ga}_{0.63}\text{N}$ photocathode used in solar-blind image intensifiers, which is efficiently characterized by MTF, is mainly governed by electron lateral diffusion within this photocathode. As key parameters of a photocathode, emission layer thickness T_e , diffusion length L_d , optical absorption coefficient α , and recombination velocity at back-interface V_b , have a significant influence on electron lateral diffusion. To improve the resolution, it is fundamental to study this dependence of MTF on these parameters. As a matter of course, by establishing the MTF model of transmission-mode varied-doping $\text{Al}_{0.37}\text{Ga}_{0.63}\text{N}$ photocathode, we have calculated and comparatively researched both MTF of transmission-mode varied-doping and uniform-doping photocathodes. Computational results show that a transmission-mode varied-doping $\text{Al}_{0.37}\text{Ga}_{0.63}\text{N}$ photocathode has a potential in achieving both high resolution and high quantum efficiency, compared with its uniform-doping counterpart. In the meantime, it is crucial to make a compromise between high resolution and high quantum efficiency in the fabrication of a transmission-mode varied-doping $\text{Al}_{0.37}\text{Ga}_{0.63}\text{N}$ photocathode.

Acknowledgements

This work was supported by Shandong Provincial Natural Science Foundation (Grant No. ZR2019MF010).

References

- [1] T. Kinoshita, T. Obata, H. Yanagi, S. Inoue, *Appl. Phys. Lett.* **102**, 012105 (2013).
- [2] H. Angerer, D. Brunner, F. Freudenberg, O. Ambacher, M. Stutzmann, *Appl. Phys. Lett.* **71**, 1504 (1997).
- [3] D. B. Li, K. Jiang, X. J. Sun, C. L. Guo, *Adv. Opt. Photonics* **10**(1), 45 (2018).
- [4] G. H. Hao, F. Shi, H. C. Cheng, B. Ren, B. K. Chang, *Appl. Opt.* **54** (10), 2572 (2015).
- [5] R. Adhikari, T. Li, G. Capuzzo, A. Bonanni, *Appl. Phys. Lett.* **108**, 022105 (2016).
- [6] S. F. Fan, Z. X. Qin, C. G. He, M. J. Hou, X. Q. Wang, B. Shen, W. Li, W. Y. Wang, D. F. Mao, P. Jin, J. C. Yang, P. Dong, *Opt. Express* **21**(21), 24497 (2013).
- [7] N. Atanov, Y. Davydov, V. Glagolev, V. Tereshchenko, D. Nechaev, S. Ivanov, V. Jmerik, *IEEE T. Nucl. Sci.* **67**(7), 1760 (2020).
- [8] Y. D. Chen, H. L. Wu, E. Han, G. L. Yue, Z. M. Chen, Z. S. Wu, G. Wang, H. Jiang, *Appl. Phys. Lett.* **106**, 162102 (2015).
- [9] N. A. Sanford, L. H. Robins, A. V. Davydov, A. Shapiro, D. V. Tsvetkov, A. V. Dmitriev, S. Keller, U. K. Mishra, S. P. DenBaars, *J. Appl. Phys.* **94**, 2980 (2003).
- [10] S. B. Li, T. Zhang, J. Wu, Y. J. Yang, Z. M. Wang, Z. M. Wu, Z. Chen, Y. D. Jiang, *Appl. Phys. Lett.* **102**, 062108 (2013).
- [11] G. H. Tang, F. Yan, X. L. Chen, W. K. Luo, *Appl. Opt.* **57**(27), 8060 (2018).
- [12] G. H. Hao, Y. J. Zhang, M. C. Jin, C. Feng, X. L. Chen, B. K. Chang, *Appl. Surf. Sci.* **324**, 590 (2015).
- [13] G. H. Tang, F. Yan, X. L. Chen, *Mat. Sci. Semicon. Proc.* **118**, 105210 (2020).
- [14] Z. S. Lv, L. Liu, X. Y. Zhang, F. F. Lu, J. Tian, *Photon. Nanostruct.* **43**, 100885 (2021).
- [15] G. H. Hao, B. K. Chang, F. Shi, J. J. Zhang, Y. J. Zhang, X. L. Chen, M. C. Jin, *Appl. Opt.* **53**(17), 3637 (2014).
- [16] Y. J. Ji, J. P. Wang, Y. W. Liu, *Chinese Phys. B* **27**(10), 106102 (2018).
- [17] X. Q. Fu, Y. Li, Z. M. Li, C. W. Zhang, X. H. Wang, *Appl. Surf. Sci.* **416**, 385 (2017).
- [18] C. Feng, Y. J. Zhang, J. Liu, Y. S. Qian, X. X. Liu, F. Shi, H. C. Cheng, *Appl. Opt.* **56**(32), 9044 (2017).
- [19] J. J. Zou, Y. J. Zhang, W. J. Deng, X. C. Peng, S. T. Jiang, B. K. Chang, *Appl. Opt.* **54**(28), 8521 (2015).
- [20] X. H. Wang, M. B. Wang, Y. L. Liao, L. F. Wang, Q. P. Ban, X. Zhang, Z. Y. Wang, S. B. Zhang, *J. Mater. Chem. C*, **9**, 13013 (2021).
- [21] R. U. Martinelli, D. G. Fisher, *Proc. IEEE.* **62**(10),

1339 (1974).

[22] G. H. Hao, M. Z. Yang, B. K. Chang, X. L. Chen,
J. J. Zhang, X. Q. Fu, *Appl. Opt.* **52**(23), 5671 (2013).

[23] J. F. Muth, J. D. Brown, M. A. L. Johnson, Z. H. Yu,
R. M. Kolbas, J. W. Cook, J. F. Schetzina, *MRS
Internet J. Nitride Semicond. Res.* **4S1**, G5.2 (1999).

* Corresponding author: whgssm@163.com